Planta (1998) 204: 506–514

Planta
© Springer-Verlag 1998

Structure and DNA methylation pattern of partially heterochromatinised endosperm nuclei in *Gagea lutea* (Liliaceae)

Jiří Bůžek[1], Irma Ebert[2], Monica Ruffini-Castiglione[3], Jiří Široký[1], Boris Vyskot[1], Johann Greilhuber[2]

[1]Institute of Biophysics, Czech Academy of Sciences, Královopolská 135, 612 65 Brno, Czech Republic
[2]Department of Systematic Karyology and Embryology, Institute of Botany, University of Vienna, Rennweg 14, A-1030 Wien, Austria
[3]Department of Botanical Sciences, University of Pisa, Via L. Ghini 5, I-56126 Pisa, Italy

Received: 24 April 1997 / Accepted: 28 July 1997

Abstract. Pentaploid endosperm nuclei in certain *Gagea* species exhibit large masses of sticky and dense chromatin, not observed in somatic nuclei. These heterochromatin masses most probably stem from the triploid chalasal polar nucleus of the embryo sac, thus representing an example of facultative heterochromatinisation in plants. In the present investigation, we studied the nuclei in *Gagea lutea* (L.) Ker-Gawl. endosperm tissue. The position of the heterochromatin in interphase nuclei was observed by confocal laser scanning microscopy (CLSM) and the DNA methylation status of the euchromatin and heterochromatin was analysed by immunolabelling with an antibody raised against 5-methylcytosine (anti-5-mC). In young endosperms, heterochromatin was relatively dispersed, occupying some peripheral and inner parts of the nuclei. In a later endosperm development, the nuclei became smaller and more pycnotic, and the heterochromatin masses were placed predominantly near the nuclear periphery. The distribution of anti-5-mC labelling on the heterochromatic regions was unequal: some parts appeared hypermethylated while other parts were, like the euchromatin, not labelled. During mitosis, the labelling intensity of all the chromosomes was approximately the same, thus indicating that there are no cytologically detectable methylation differences among the individual sets of chromosomes. However, differences in the anti-5-mC signal intensity along individual chromosomes were observed, resulting in banding patterns with highly positive bands apparently representing constitutive heterochromatic regions. From these results it is obvious that facultative heterochromatinisation, in contrast to constitutive heterochromatinisation, need not be strictly accompanied by a prominent DNA hypermethylation.

Key words: DNA methylation – Facultative heterochromatin – *Gagea* – Endosperm nucleus (pentaploid)

Introduction

Endosperm is an embryo-feeding tissue in seed plants. Its nuclei are a product of the fusion of a male sperm with one or more nuclei in the central cell of the embryo sac. *Gagea lutea* (Liliaceae, $2n = 72$) forms an embryo sac of the *Fritillaria* type with a triploid chalasal and a haploid micropylar polar nucleus. During the first mitosis after double fertilisation, the nuclei in the central cell fuse and form the pentaploid endosperm with one paternally and four maternally derived genomes. Geitler (1950) first described the unique structure of *Gagea lutea* endosperm nuclei. In interphase, some parts of their chromatin have a normal, decondensed structure, but others are arranged into a sticky, branching and very dense mass (heterochromatin). The occurrence of this structure is restricted only to the endosperm nuclei of this and several related (but not all) *Gagea* species. In older endosperms, the nuclei become smaller and the heterochromatin is even more pycnotic. At mitosis, the relaxed parts of the nucleus are the first to form chromosomes (in early prophase), while the dense parts break up into single chromosomes only in late prophase (Geitler 1950).

Romanov (1961), based on his embryological investigations on other *Gagea* species, attributed the endosperm heterochromatin masses to the three maternal genomes which formed the chalasal polar nucleus in the embryo sac. This polar nucleus, although triploid, is much smaller than the haploid micropylar polar nucleus, and thus much more dense. After the fusion of these nuclei with the sperm, the dense structure of the chalasal polar nucleus remains preserved in endosperm nuclei as the heterochromatin. This hypothesis was supported by investigations of fertilisation in *G. chomutovae*. In this species the triploid chalasal polar nucleus

Abbreviations: anti-5-mC = anti-5-methylcytosine antibody; CLSM = confocal laser scanning microscopy; DAPI = 4′,6-diamidino-2-phenyl-indole; FITC = fluorescein-isothiocyanate

Correspondence to: B. Vyskot; E-mail: vyskot@ibp.cz; Tel/Fax: 420 (5) 41240500

possesses a decondensed structure and its volume is three times higher than the micropylar haploid nucleus. Consequently, no large endosperm heterochromatin masses are found in this species (Romanov 1961; Geitler 1963).

It is generally accepted that cytosine methylation plays an important role in transcriptional inactivation of genes. Hypermethylation of DNA also has striking effects on the chromatin structure. It causes a lower sensitivity to nuclease cleavage, indicating differences in higher-order chromatin folding compared with undermethylated regions (Selker 1990). The methylation state of a particular DNA region thus reflects alternative structural states of the corresponding chromatin and DNA hypermethylation can be an accompanying or even causative phenomenon in the process of forming inactive chromatin both in mammals (Adams 1996) and in plants (Espinas and Carballo 1993). In eukaryotic chromosomes, heterochromatic regions were found to have a higher 5-methylcytosine content as shown by in situ immunolabelling (Barbin et al. 1994; Ruffini-Castiglione et al. 1995), indicating that the DNA hypermethylation could be detected at the cytological level.

The aim of this work was to describe the structure of *Gagea lutea* endosperm nuclei during its development using confocal laser scanning microscopy (CLSM) and to follow the DNA methylation patterns in various stages of the cell cycle in order to determine whether the bulk of DNA in the dense chromatin regions is hypermethylated.

Materials and methods

Plant material. Immature fertilised ovaries of wild-growing *Gagea lutea* (L.) Ker-Gawl. plants were collected at Prater meadows, Vienna, Austria, fixed in methanol:acetic acid (3:1, v/v) and kept in 96% ethanol at −20 °C until used.

Slide preparation for CLSM. Immature seeds were extirpated from the ovaries and transferred into a drop of Soerensen's phosphate buffer (50 mM, pH 6.8) on poly-L-lysine-coated slides. Seeds were opened and the intact endosperm, endosperm cells (in older endosperms) and cells from the integuments were released. The endosperm tissue was further divided into pieces containing several nuclei. All these manipulations were done under a dissection microscope using fine needles. The liquid was carefully exchanged for 10 $\mu g \cdot \mu l^{-1}$ acridine orange (Sigma, Deisenhofen, Germany) in the same buffer and the slides were left in a moist chamber for 15 min at room temperature. The drop of staining solution was then washed out and replaced with the phosphate buffer which served as a mounting medium. To preserve the three-dimensional structure of nuclei, samples were not allowed to dry out at any time. Four small drops of rubber cement were applied to coverslips to make spacers. The slides were covered with these coverslips and sealed with rubber cement.

Slide preparation for immunolabelling. Immature seeds were transferred into a drop of 45% acetic acid on poly-L-lysine-coated slides. The preparation of endosperm and integument nuclei was the same as described above. Other tissues were then removed together with an excess of liquid and a coverslip was applied with a slight pressure. The coverslips were then removed using the dry-ice technique. The quality of the preparations and the stage of the cell cycle were checked using phase-contrast microscopy. Before use, the preparations were stored desiccated for at least one week at −20 °C.

Immunolabelling. The preparation and characterisation of a mouse monoclonal antibody against 5-methylcytosine (anti-5-mC) has already been described (Podestá et al. 1993). For immunolabelling, a modified protocol of Frediani et al. (1996) was used. Preparations were treated with 5 $\mu g \cdot ml^{-1}$ RNase in 2 × SSC (saline sodium citrate buffer 0.3 M NaCl, 0.03 M sodium citrate) for 2 h. Slides were postfixed in ethanol:acetic acid (3:1, v/v) for 30 min, dehydrated in 100% ethanol and air-dried. Denaturation of DNA was carried out in a mixture of 0.07 N sodium hydroxide:100% ethanol (7:3, v/v) for 30 s. Slides were then dehydrated in an ascending ethanol series (50, 70 and 100%, 5 min each) and air-dried. The slides were blocked in phosphate-buffered saline (PBS) supplemented with 1% (w/v) BSA and 0.5% (v/v) Tween-20 (solution A) and the monoclonal anti-5-mC, diluted 1:1000 in solution A, was applied to the slides. Incubation was carried out for 1 h in a moist chamber at room temperature, and the slides were washed 3 × 10 min in solution A without BSA. The anti-5-mC was visualised using an anti-mouse secondary antibody-fluorochrome conjugate, either a sheep fluorescein-isothiocyanate (FITC)-conjugated antibody (Sigma; working concentration 8.6 μg protein $\cdot ml^{-1}$) or a goat rhodamine-conjugated antibody (Boehringer Mannheim, Germany; working concentration 20 μg protein $\cdot ml^{-1}$). Slides were then washed as previously described and mounted in Vectashield (Vector Laboratory, Burlingame, Calif., USA) with 4′,6-diamidino-2-phenylindole (DAPI; 1 $\mu g \cdot ml^{-1}$) or DAPI/propidium iodide mixture (0.5 $\mu g \cdot ml^{-1}$ each). As controls, the standard procedure without an application of the anti-5-mC (a negative control), and an immunolabelling with a mouse anti-DNA (Boehringer Mannheim; working concentration 1.25 μg protein $\cdot ml^{-1}$, a positive control) were used.

Image acquisition and processing. The CLSM analyses were done on a Sarastro 2000 confocal laser scanning microscope (Molecular Dynamics, Sunnyvale, Calif., USA) and images were processed using the Indigo workstation (Silicon Graphics) with ImageSpace software (Molecular Dynamics). In the case of whole nuclei stained with acridine orange, only the DNA fluorescence (green, 488 nm excitation/510 nm emission filter) could be scanned by CLSM, because the RNA fluorescence (red, 488 nm excitation/535 nm emission filter) faded quickly when excited by the laser beam. Therefore, single-focusing-plane images of the corresponding nuclei containing both DNA and RNA fluorescence were done using a conventional fluorescence microscope and pseudocoloured as faint grey (DNA) and bright grey (RNA) to show the nucleoli. Standard epifluorescence-microscope imaging of immunolabelled preparations was performed on an Olympus AX-70. Images were captured by a CCD camera (Imac-530, Compulog, Böblingen, Germany) and processed using the ISIS Software (MetaSystems, Sandhausen, Germany). The colour images were converted to black-and-white and printed using the Paint Shop Pro software (JASC, Minnetonka, Minn., USA) and a Mitsubishi (Tokyo, Japan) CP-D1 Digital Printer. The 3-dimensional fluorescence intensity plots of immunolabelled nuclei were created using the Imagespace software run on the Indigo workstation.

Measurements of nuclei. To quantify the nuclear volume changes during the endosperm development and to compare the DNA content between endosperm and somatic nuclei, the nuclear volumes and DNA fluorescence intensities in the nuclei scanned by CLSM were measured. The sections were separated by an equal step size (2 μm) and their number per nucleus was 10 in most cases. In each variant, 20 endosperm and 50 somatic nuclei from at least two different preparations were measured. Computations of nuclear volumes and DNA fluorescence were based upon the characteristics of all pixels (imaging units) representing the DNA-specific acridine orange fluorescence in a nucleus: volume was derived from the total number of voxels (voxel = pixel area × step size), the DNA fluorescence intensity was expressed in arbitrary

Table 1. Characteristics of individual stages in the development of *Gagea lutea* endosperm

Stage	Approximate dimensions of immature seeds (length × width, mm)	Appearance of endosperm tissue	Approximate number of nuclei per endosperm
1	3–4 × 2 or less	single layer of nuclei in syncytium, large central vacuole	16–100
2	4–5 × 2–3	the same as at stage 1	100–200
3	4–5 × 3	cellularisation, starch accumulation	many hundreds

units as the sum of pixel intensities. To differentiate the nuclei according to the phase of the cell cycle, computer-assisted bivariate (volume + fluorescence intensity) K-means cluster analysis was initially applied to each dataset. The nuclei of the same tissue and developmental stage were grouped into two clusters, assuming that these clusters represent the nuclei at G1 and G2 phases. For each variable, the mean value and standard error were determined. The volumes and fluorescence intensities were then compared between the endosperm nuclei at different stages of development for both G1 and G2 phases, using the Student's *t*-test.

Results

Structure of endosperm nuclei. The endosperm studied ranged from the very early (approx. four divisions after fertilisation, 16 nuclei per endosperm) to late (several hundreds of cells) developmental phases. To characterise the appearance of tissues and nuclei during endosperm development, three typical stages were selected and described (Table 1). At the beginning of its development (stages 1 and 2), the endosperm was typically of the nuclear type (syncytium), with a large central vacuole and a single layer of nuclei on the surface. In later development (stage 3), cell walls were formed among the nuclei, the central vacuole disappeared and a high number of starch grains were observed within the endosperm cells.

At stage 1, endosperm nuclei had the largest volume. They were relatively flat and contained heterochromatin in the form of elongated and branching parts both at the periphery and in the centre of nuclei. Centrally positioned heterochromatin masses were always found to be in contact with large nucleoli (Fig. 1a). Euchromatic parts of the nuclei, in contrast to the chromatin present in a diploid somatic nucleus (Fig. 1d), possessed a highly relaxed structure consisting of fine chromatin fibres. At stage 2 (endosperms immediately before starch accumulation), the nuclei became smaller, oval-shaped and the density of the heterochromatin increased (Fig. 1b). Heterochromatin branches in these nuclei tended to fuse and were placed near the nuclear periphery. The measurements of endosperm nuclei (Table 2) showed a statistically significant decrease in the nuclear volume of older endosperms (stage 3). On the other hand, the DNA fluorescence intensities of nuclei at stages 1 and 3 were approximately the same, indicating the overall chromatin condensation during endosperm development (Table 2). The nuclei at stage 3 were almost round-shaped, and the heterochromatin was apparent as a few (usually one or two) highly compact bodies, located at the nuclear periphery. The nucleoli were no longer observed at this late stage (Fig. 1c).

The chromatin mass in the diploid somatic interphase nuclei from integuments was equally distributed throughout the whole nuclear volume (Fig. 1d). The chromocentres, visible by light microscopy (Geitler 1950), were not observed after acridine orange staining and fluorescence microscopy. The mean DNA fluorescence intensity per somatic nucleus was about one-half to one-third of the value measured in the endosperm (Table 2). These values are in accordance with the expected ploidy levels of somatic and endosperm nuclei ($2n$ and $5n$, respectively).

Distribution of 5-methylcytosine-rich regions on interphase nuclei. The interphase endosperm nuclei at each of the three selected stages and somatic nuclei were labelled with the anti-5-mC (Fig. 2). The immunolabelling showed that the heterochromatin generally displayed a stronger signal than the euchromatin. However, the signal distribution over the heterochromatin was strikingly unequal in each of the three stages. The most intensive labelling was always concentrated into discrete spots or areas on heterochromatin branches, while the other heterochromatic parts were, like the euchromatin, weakly labelled or unlabelled (Fig. 2a,b). This unequal labelling pattern is demonstrated in a quantitative way in Fig. 3 as the DNA and anti-5-mC fluorescence intensity plots. In Fig. 3a, for example, the largest region of heterochromatin positioned approximately in the middle of the nucleus shows a low or no anti-5-mC signal, as in the euchromatic parts. In older endosperm nuclei, the signal was more intensive and uniform, obviously due to the more pycnotic heterochromatin in these nuclei (Figs. 2c, 3b). The anti-5-mC labelling on diploid somatic nuclei displayed a dot-like pattern, with sites of an enhanced signal, probably corresponding to chromocentres. The chromocentres were, however, not distinguishable from the other nuclear mass in the DAPI-stained nuclei, as in the case of acridine orange staining (Fig. 2d). The control anti-DNA antibody labelling showed a signal distribution on the nuclei corresponding to the DNA (DAPI fluorescence) staining (Fig. 2e).

Anti-5-methylcytosine antibody labelling during mitosis. The anti-5-mC labelling analysis was also performed in various phases of mitosis in young endosperm (stage 1). The prophase chromosome formation took place first in

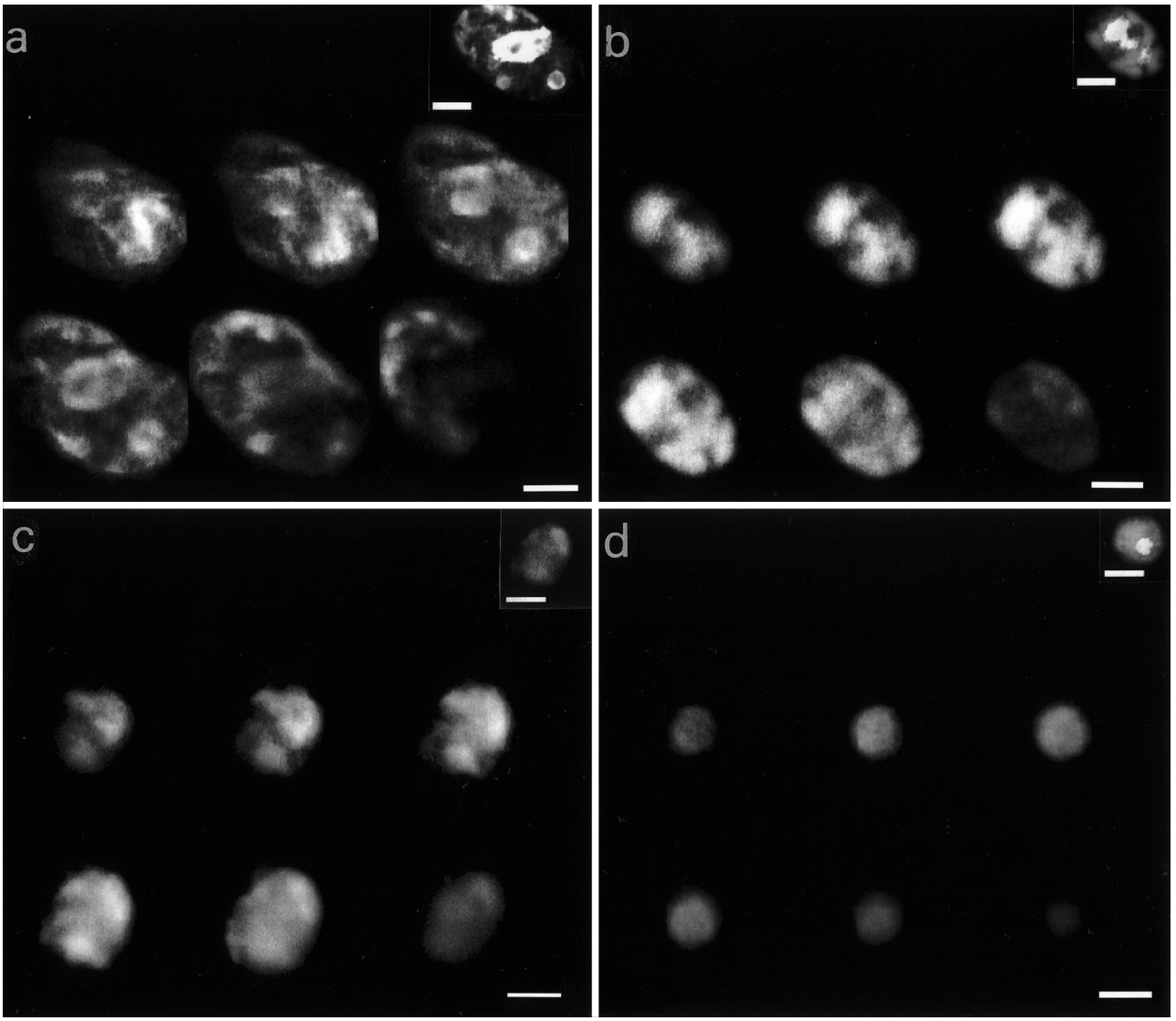

Fig. 1a–d. Three-dimensional structure of *Gagea lutea* endosperm nuclei, stained with acridine orange. Sets of six CLSM sections of nuclei at developmental stages 1 (**a**), 2 (**b**), and 3 (**c**) are presented, showing the arrangement and appearance of the dense and relaxed parts of their chromatin. A diploid nucleus from integuments (**d**) is also shown for comparison. The sections are separated by 2 μm. In various cases the CLMS photomultiplier gain setting was different in order to distinguish the heterochromatin properly. In the upper right corners are shown the same nuclei observed at a single focusing plane by the standard epifluorescence microscope: DNA (*faint*) and RNA (*bright*) fluorescences are superimposed to show the position of nucleoli. Bars = 10 μm

the euchromatin, while the heterochromatin persisted to prometaphase. In prometaphase, the heterochromatin parts disappeared and formed normally shaped chromosomes. The labelling patterns of these chromosomes were similar to those of the other chromosomes not attached to the persisting heterochromatin parts, that were considered to form the euchromatin. In both cases, distinct labelled bands on the chromosomes were found and the overall intensity of labelling was similar throughout the whole prometaphase nucleus (Fig. 4a).

Table 2. Average volumes and DNA fluorescence intensities (± SD) of acridine orange-stained endosperm and somatic nuclei. The values compared by the individual *t*-tests are marked by identical letters

Nuclei	Phase of cell cycle	Average volume [μm^3]	Average intensity of fluorescence [arbitrary units]
Endosperm, stage 1	G1	7471 ± 2208[a]	3056948 ± 424963[c]
	G2	11553 ± 1807[b]	7522664 ± 1256112[d]
Endosperm, stage 3	G1	4339 ± 761[a]	2799510 ± 685964[c]
	G2	5767 ± 1132[b]	7611664 ± 907986[d]
Somatic, from integuments	G1	1987 ± 738	1427789 ± 292324
	G2	3946 ± 758	2725242 ± 352294

[a]Differences are significant ($0.001 < P < 0.01$)
[b]Differences are significant ($P < 0.001$)
[c]Differences are not significant ($0.2 < P < 0.4$)
[d]Differences are not significant ($0.5 < P$)

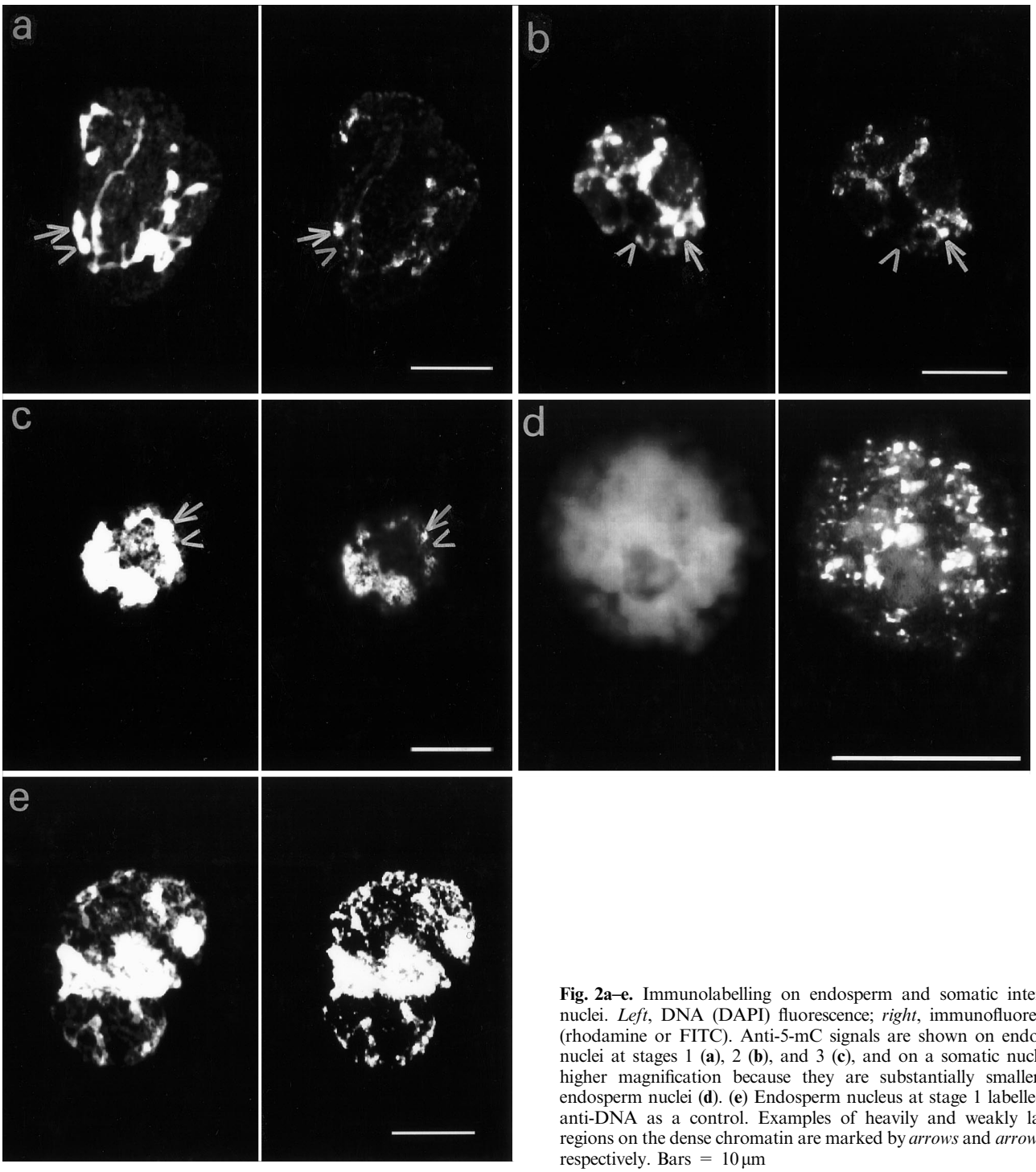

Fig. 2a–e. Immunolabelling on endosperm and somatic interphase nuclei. *Left*, DNA (DAPI) fluorescence; *right*, immunofluorescence (rhodamine or FITC). Anti-5-mC signals are shown on endosperm nuclei at stages 1 (**a**), 2 (**b**), and 3 (**c**), and on a somatic nucleus in higher magnification because they are substantially smaller than endosperm nuclei (**d**). (**e**) Endosperm nucleus at stage 1 labelled with anti-DNA as a control. Examples of heavily and weakly labelled regions on the dense chromatin are marked by *arrows* and *arrowheads*, respectively. Bars = 10 μm

A structure strongly autofluorescent at rhodamine excitation/emission wavelength in Fig. 4a (right, marked by an arrow) was subsequently recognised as a nucleolus (using the silver nitrate staining, data not shown), which remained attached to the prometaphase nucleus and covered the largest part of the persisting heterochromatin.

The anti-5-mC immunolabelling in anaphase resulted in an approximately uniform signal distribution in all the chromosomes (Fig. 4b). In telophase, the dense

Fig. 3a,b. Three-dimensional fluorescence intensity plots of two randomly selected nuclei at stages 1 (**a**) and 3 (**b**). The images show the measured nuclei; the graphs below show distributions of fluorescence intensities in the corresponding nuclei: *left*, DNA (DAPI) fluorescence; *right*, anti-5-mC signal (rhodamine fluorescence) in each case. x and y axes, horizontal nuclear dimensions (μm); z axis, fluorescence intensity (arbitrary units). Fluorescence intensities are also presented as different levels of grey pseudocolouring. Note conspicuous differences in the anti-5-mC signal intensity on the heterochromatic (i.e., highly DAPI-positive) regions

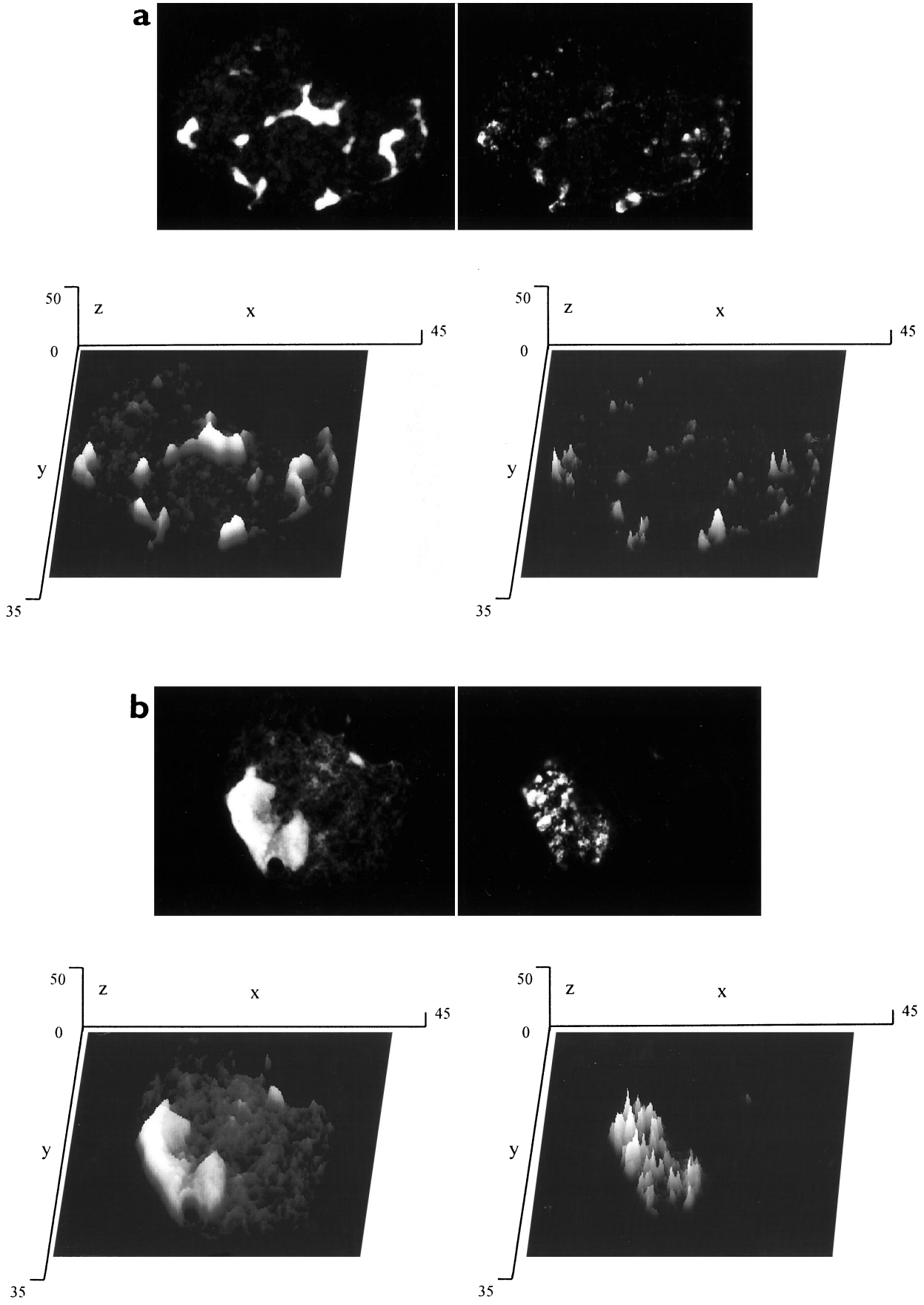
a
50
z
x
45
0
y
35
50
z
x
45
0
y
35
b
50
z
x
45
0
y
35
50
z
x
45
0
y
35

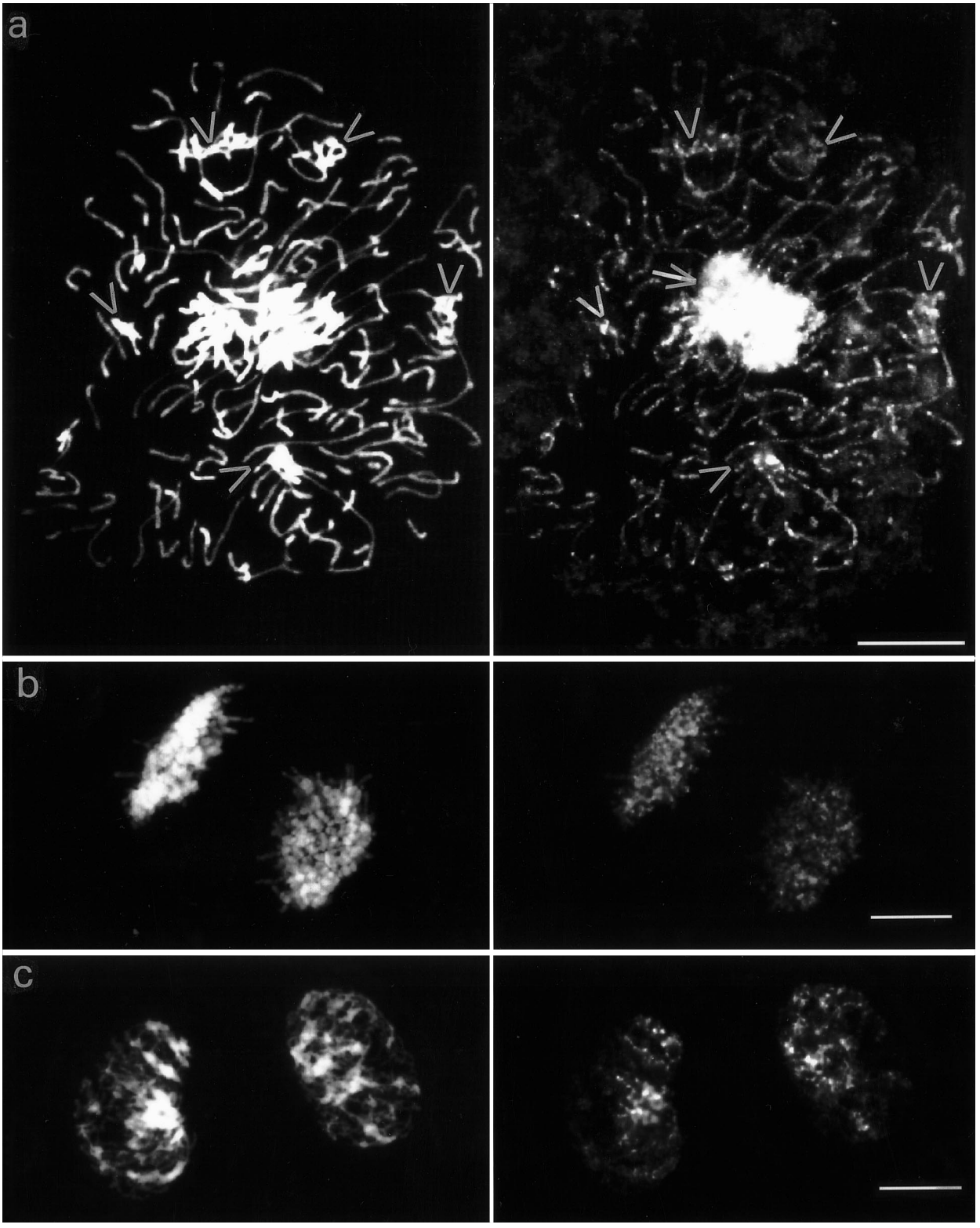

Fig. 4a–c. Anti-5-mC-labelled endosperm nuclei at stage 1 in different phases of mitosis. *Left*, DNA (DAPI) fluorescence; *right*, anti-5-mC signal (rhodamine fluorescence). Prometaphase (**a**), anaphase (**b**), and telophase (**c**) nuclei are shown. The nucleolus in **a** is marked by an *arrow*; parts of heterochromatin, dividing into chromosomes, are indicated by *arrowheads*. Bars = 10 μm

chromatin masses were formed in a mirror-symmetrical manner between the two daughter nuclei. The anti-5-mC generated bright fluorescence spots on the heterochromatin, while the rest of chromatin remained weakly labelled (Fig. 4c).

Discussion

The structural variation of plant cell nuclei and chromosomes has been extensively studied by light-microscopical means (Heitz 1932; Tschermak-Woess 1963), by chromosome-banding methods (e.g. Berg and Greilhuber 1992) and by more-recent techniques, such as fluorescence in-situ hybridisation (Bauwens et al. 1991; Rawlins et al. 1991). Factors determining the nuclear architecture involve the amount and distribution of constitutive heterochromatin (Tschermak-Woess 1963), genome size (Barlow 1977) and the position of individual chromosomes within the nucleus (Heslop-Harrison and Bennett 1990). Among different cell types of a plant body, often no prominent differences in nuclear structure are found, although there are some exceptions, e.g. highly endopolyploid (endoreduplicated) nuclei, especially in antipodals, endosperm haustoria and embryo suspensor, where chromatin bundles or even polytene chromosomes are formed (for a review, see Nagl 1985). The endosperm nuclei are generally more voluminous than diploid somatic nuclei, but their structure is usually not altered (Enzenberg 1961).

The present study on nuclear structure and mitosis in *Gagea lutea* endosperm confirms the results of Geitler (1950) and Romanov (1961). The measurements of fluorescence intensity and approximate chromosome numbers in prometaphase both indicate that the nuclei are pentaploid, possessing 180 chromosomes. The occurrence of the dense chromatin mass thus cannot be attributed to DNA endoreduplication. The three chromosome sets, present in the chalasal polar nucleus and further in the endosperm, undergo normal mitosis, but remain condensed in interphase; they can thus be considered as a typical example of facultative heterochromatin. The close association of heterochromatin with the nucleoli, already observed by Geitler (1950), indicate that the rDNA sites from the heterochromatinised genomes are partially or completely active. During endosperm development, the volume of nuclei decreases, the nuclear structure becomes more compact and the nucleoli disappear. In eukaryotes, overall nuclear condensation is one of the early features of nuclei undergoing programmed cell death, apoptosis (Wyllie 1980). Apoptosis has also been observed in plant tissues of ripening fruits and seeds, during xylogenesis and somatic embryogenesis (for a review, see Greenberg 1996). Since the endosperm represents a terminally differentiated tissue which is degraded during embryo development and seed germination, the apoptosis is obviously involved in late endosperm development (Wang et al. 1996).

Heterochromatinisation is often accompanied by DNA hypermethylation (Lewis and Bird 1991). Therefore, methylation differences between the dense and relaxed chromatin regions could be expected in *G. lutea* endosperm nuclei. Our results, however, show that only a part of the heterochromatin mass contains highly methylated DNA, detectable by the anti-5-mC labelling, while the rest of heterochromatin remains predominantly unlabelled, like the euchromatin (Figs. 2, 3). In prometaphase and anaphase, where all the chromatin has approximately the same density (it is arranged into chromosomes), no overall differences in the labelling intensity among the chromosomes are apparent. Therefore, if methylation differences between the euchromatin and facultative heterochromatin exist, they are fine and not detectable by the immunocytology approach. However, methylation differences along individual chromosomes were detectable, as also described in other plant species, e.g. *Allium cepa* (Ruffini-Castiglione et al. 1995) or *Vicia faba* (Frediani et al. 1996). The 5-methylcytosine-rich chromosome bands represent the constitutive heterochromatin containing highly repetitive, non-transcribed DNA sequences. The foci of enhanced anti-5-mC signal, observed in *G. lutea* endosperm interphase nuclei, obviously represent positions of such constitutive heterochromatin on the chromosomes lying inside the dense chromatin mass (facultative heterochromatin).

At present, there are two well-described examples of cytologically observable facultative heterochromatinisation in eukaryotes: an X-chromosome inactivation in female mammals (Barr and Bertram 1949) and an inactivation of the whole paternally derived genome in diploid males of mealybugs, Coccoidea (Khosla et al. 1996). In some species of these insects, the male cells have a slightly higher 5-methylcytosine content than the female, but this is not a general rule for all the species where heterochromatinisation occurs (Nur 1990). The X-chromosome inactivation (Barr body formation) is the most striking expression of facultative heterochromatinisation in mammals (e.g. Lyon 1971). This phenomenon has also been studied by various immunocytological methods. Using the anti-5-mC immunolabelling technique, Barbin et al. (1994) and Bernardino et al. (1996) were not able to find any significant difference between the active and inactive human X-chromosomes. These results show that the overall hypermethylation of the inactive X-chromosome does not occur, but a specific methylation of X-chromosome-linked DNA sequences has been revealed by molecular genetic analyses (e.g. Grant et al. 1992). A distinguished lack of histone H4 acetylation was observed on the inactive X-chromosome by immunostaining (Jeppesen and Turner 1993). This indicates that other epigenetic mechanisms, such as the deacetylation of core nucleosomal histones, can be responsible for the facultative heterochromatinisation. Although the facultative heterochromatin formation may include various mechanisms in plants and animals, the above-mentioned examples indicate that large methylation changes (detectable at the chromosomal level) do not seem to be involved in this process.

We sincerely thank Ms Renáta Hladilová for excellent technical assistance and Ms Carri Goodman for English revision. This research was supported by the Grant Agency of the Czech Republic (521/96/1717) and the Grant Agency of the Czech Academy of Sciences (A5004601).

References

Adams RLP (1996) DNA methylation. In: Bittar EE, Bittar N (eds) Principles of medical biology 5. Molecular and cellular genetics. JAI Press, Greenwich, Cohn., USA, pp 33–66

Barbin A, Montpellier C, Kokalj-Vokac N, Gibaud A, Niveleau A, Malfoy B, Dutrillaux B, Bourgeois CA (1994) New sites of methylcytosine-rich DNA detected on metaphase chromosomes. Hum Genet 94: 684–692

Barlow PW (1977) Determinants of nuclear chromatin structure in angiosperms. Ann Sci Nat (Paris) 18: 193–206

Barr ML, Bertram EG (1949) A morphological distinction between the neurones of the male and female, and the behaviour of the nucleolar satellite during accelerated nucleo-protein synthesis. Nature 163: 676–677

Bauwens S, Van Oostveldt P, Engler G, Van Montagu M (1991) Distribution of the rDNA and three classes of highly repetitive DNA in the chromatin of interphase nuclei of *Arabidopsis thaliana*. Chromosoma 101: 41–48

Berg C, Greilhuber J (1992) Cold-sensitive chromosome regions and their relation to constitutive heterochromatin in *Cestrum parqui*. Genome 35: 921–930

Bernardino J, Lamoliatte E, Lombard M, Niveleau A, Malfoy B, Dutrillaux B, Bourgeois CA (1996) DNA methylation of the X chromosomes of the human female: an in situ semi-quantitative analysis. Chromosoma 104: 528–535

Enzenberg U (1961) Beiträge zur Karyologie des Endosperms. Österr Bot Z 108: 245–285

Espinas ML, Carballo M (1993) Pulsed-field gel electrophoresis analysis of higher-order chromatin structures of *Zea mays*. Highly methylated DNA in the 50 kb chromatin structure. Plant Mol Biol 21: 847–857

Frediani M, Giraldi E, Ruffini-Castiglione M (1996) Distribution of 5-methylcytosine-rich regions in the metaphase chromosomes of *Vicia faba*. Chromosome Res 4: 141–146

Geitler L (1950) Notizen zur endomitotischen Polyploidisierung in Trichocyten und Elaiosomen sowie über Kernstrukturen bei *Gagea lutea*. Chromosoma 3: 271–281

Geitler L (1963) Morphologie und Entwicklungsgeschichte der Zelle. Fortschr Bot 25: 1–12

Grant M, Zuccoti M, Monk M (1992) Methylation of *CpG* sites of two X-linked genes coincides with X-inactivation in the female mouse embryo but not in the germ line. Nature Genet 2: 161–166

Greenberg JT (1996) Programmed cell death: a way of life for plants. Proc Natl Acad Sci USA 93: 12094–12097

Heitz E (1932) Die Herkunft der Chromozentren. Planta 18: 571–636

Heslop-Harrison JS, Bennett MD (1990) Nuclear architecture in plants. Trends Genet 6: 402–405

Jeppesen P, Turner BM (1993) The inactive X chromosome in female mammals is distinguished by a lack of histone H4 acetylation a cytogenetic marker for gene expression. Cell 74: 281–289

Khosla S, Kantheti P, Brahmachari V, Chandra HS (1996) A male-specific nuclease-resistant chromatin fraction in the mealybug *Planococcus lilacinus*. Chromosoma 104: 386–392

Lewis J, Bird A (1991) DNA methylation and chromatin structure. FEBS Lett 285: 155–159

Lyon M (1971) Possible mechanisms of X chromosome inactivation. Nature New Biol 232: 229–233

Nagl W (1985) Chromatin organization and the control of gene activity. Int Rev Cytol 94: 21–56

Nur U (1990) Heterochromatinisation and euchromatinisation of whole genomes in scale insects (Coccoidea, Homoptera). Development (Suppl): 29–34

Podestá A, Ruffini-Castiglione M, Avanzi S, Montagnoli G (1993) Molecular geometry of antigen binding by a monoclonal antibody against 5-methylcytosine. Int J Biochem 25: 929–933

Rawlins DJ, Highett MI, Shaw PJ (1991) Localisation of telomeres in plant interphase nuclei by in situ hybridisation and 3D confocal microscopy. Chromosoma 100: 424–431

Romanov ID (1961) The origin of the unique structure of endosperm nuclei in *Gagea*. Dokl Bot Sci Sect 141: 188–190

Ruffini-Castiglione M, Giraldi E, Frediani M (1995) The DNA methylation pattern of *Allium cepa* metaphase chromosomes. Biol Zentralbl 114: 57–66

Selker EU (1990) DNA methylation and chromatin structure: a view from below. Trends Biochem Sci 15: 103–107

Tschermak-Woess E (1963) Strukturtypen der Ruhekerne von Pflanzen und Tieren (Protoplasmatologia V/1). Springer, Wien

Wang M, Oppedijk BJ, Lu X, Van Duijn B, Schilperoort RA (1996) Apoptosis in barley aleurone during germination and its inhibition by abscisic acid. Plant Mol Biol 32: 1125–1134

Wyllie AH (1980) Cell death: the significance of apoptosis. Int Rev Cytol 68: 251–306